Research Article

Journal of PeptideScience

Received: 24 July 2009 Revised: 21 November 2009 Accepted: 23 November 2009 Published online in Wiley Interscience:

(www.interscience.com) DOI 10.1002/psc.1206

Nanofiber formation of amphiphilic cyclic tri-β-peptide

Yusuke Ishihara and Shunsaku Kimura*

A novel amphiphilic cyclic peptide composed of two β-glucosamino acids and one *trans*-2-aminocyclohexylcarboxylic acid was synthesized and investigated on assembly formation. The cyclic tri-β-peptide was self-assembled into rodlike crystals or nanofibers depending on preparative conditions. The rodlike crystals showed a layer spacing of 4.8 Å along the long axis, and columnar spacings of 10.8 and 21.5 Å by electron diffraction analysis along the short axis. The former confirms the columnar structure upon molecular stacking, and the latter indicates triple bundle formation of the columnar assemblies. Fourier transform infrared (FT-IR) measurement of the fibrous assembly showed formation of homogeneous hydrogen bonds among amide groups, also supporting the molecular stacking of cyclic β-peptides. Straight nanofibers with uniform diameter were also uniquely obtained. Copyright © 2010 European Peptide Society and John Wiley & Sons, Ltd.

Keywords: β-amino acid; cyclic peptide; self-assembly; nanofiber; amphiphilic peptide

Introduction

Organic nanosize fibrous molecular assemblies have attracted much attention with regard to functional materials in the fields of materials science [1–4] and biomaterials [5–9], etc. Peptides have been frequently used for the nanofiber preparations because peptides tend to associate together via intermolecular hydrogen bonds like β-sheet structure [10–19]. Size and surface properties of the peptide assemblies are adjustable for various materials by proper design of the primary structure. [20] Surface design of peptide assemblies was also reported with peptide nanotubes (PNTs), which are generally characterized by molecular stacking of cyclic peptides of α- [21–25] and β-amino acids [26–28] via intermolecular hydrogen bonds with the formation of a well-defined pore inside. The pore size is controllable precisely by changing the number of constituent amino acids of the cyclic peptides.

Further, PNTs composed of β-amino acids are unique in exhibiting a strong dipole moment along the nanotube axis. We have prepared several cyclic β-peptides to investigate the nanotube formation and its functionalization. We have chosen *trans*-2-aminocyclohexylcarboxylic (ACHC) acid and β-glucosamino acid (GA) as components of cyclic β-peptides because the cyclic side chains promote molecular stacking to yield long and stable nanotubes due to the planar geometry. However, PNTs have a strong tendency to associate together to form thick bundles, probably because the dipole–dipole interaction between PNTs attracts them to take an antiparallel orientation, leading to the formation of thick bundles [28–30]. Control of the PNT number in the bundles to keep it small is therefore challenging.

One typical way to control the bundle size is to use the leucine-zipper motif in addition to introduction of complementary ionic groups to each helical chain as found in the coiled-coil structure [31–33]. However, these molecular designs would not be applicable to PNTs, because they influence the molecular stacking manner of cyclic peptides. The other way is to be endowed with an amphiphilic property [20,34,35]. In the present study, we tried to control the association number of PNTs in the bundle by using an amphiphilic cyclic tri-β-peptide (CP2).

Here we have synthesized an amphiphilic CP2 to study the PNT and the bundle formation. As shown in Figure 1(a), CP2 is composed of two hydrophilic GAs and one hydrophobic ACHC. CP2 is expected to stack together to form PNT, and in aqueous environment three PNTs should associate reasonably well with the hydrophobic ACHC residue facing inward and the two hydrophilic GA residues pointing outward (Figure 1(b–d)). In our previous report, CP2 of ACHC produced a crystal of PNTs aligned in a parallel manner. The parallel orientation is considered to be due to the interdigitation of cyclohexyl side chains between PNTs. If CP2 would hold this unique property of ACHC, three PNTs in the bundle should possess an extremely large dipole. The morphology and structure of molecular assemblies of CP2 are thus studied here mainly by transmission electron microscopy (TEM) observations by changing the peptide concentrations.

Materials and Methods

Spectroscopic Measurements

NMR spectra were recorded with a Bruker DPX-400 spectrometer. FAB mass spectra were obtained on a JEOL JMS HX-110A spectrometer. FT-IR was performed with a Nicolet 6700 FT-IR spectrometer.

Structure Calculation

Geometry optimization was carried out by the CAChe software (Fujitu Co., Japan), the molecular Mechanics program 2 (MM2), and the semi-empirical Austin Model (AM1) method in the MOPAC 2002 package.

* *Correspondence to: Shunsaku Kimura, Department of Material Chemistry, Graduate School of Engineering, Kyoto University, Kyoto-Daigaku-Katsura, Nishikyo-ku, Kyoto 615-8510, Japan. E-mail: shun@scl.kyoto-u.ac.jp*

Department of Material Chemistry, Graduate School of Engineering, Kyoto University, Kyoto-Daigaku-Katsura, Nishikyo-ku, Kyoto 615-8510, Japan

Journal of PeptideScience

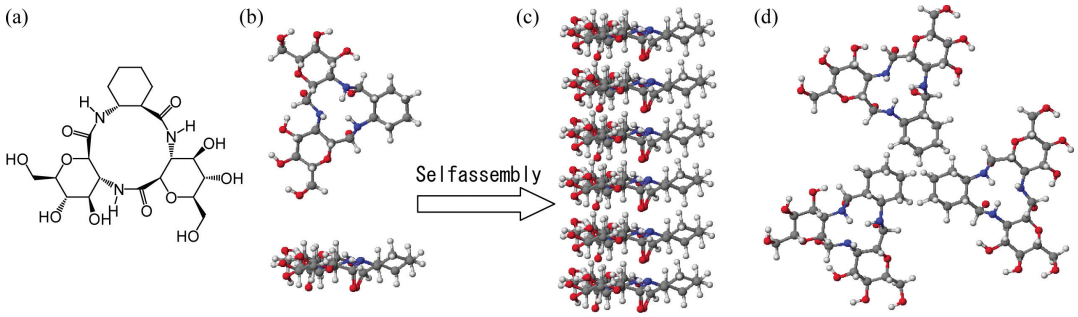

Figure 1. (a) The cyclic tri-β-peptide CP2 is composed of two hydrophilic GAs and one hydrophobic ACHC. (b) Geometry-optimized structure of cyclic tri-β-peptide, CP2. (c) (Top panel: top view, bottom panel: side view), schematic illustration of PNT from CP2. (d) Scheme of association of three CP2 molecules based on the amphiphilic structure. Hydrophobic cyclohexyl side chains are aligned in a straight form to make the surface hydrophobic. The other surface is hydrophilic, thus leading to association of PNTs.

Optical Microscopy

Optical microscopy was performed with an Olympus IX70. A dispersion of crystals was placed between a slide glass and a cover glass, and observed under cross-Nicol configuration. The sensitive tint plate was set between the polarizers.

TEM and Electron Diffraction

The images and diffraction were taken with JEOL JEM-2000EXII (JEOL, Japan) at an accelerating voltage of 100 kV. A drop of the sample was dried on a carbon-coated Cu grid.

The electron diffraction diagrams were obtained in the microdiffraction mode. The distance in the diffractions was calibrated with the (111) diffraction ring of evaporated Au particles.

Scanning Electron Microscope (SEM)

The image was taken with Keyence VE-8800 at an accelerating voltage of 5 kV. A drop of the sample was dried on a Au-coated glass.

Synthesis of Cyclic Peptide

Boc-(GA(OAc)-ACHC)-OCH$_2$C$_6$H$_5$ (1)

p-TosOH H-ACHC-OBn [36] (470 mg, 1.16 mmol), Boc-GA(OAc)-OH [37] (437 mg, 1.05 mmol), and HATU (526 mg, 1.39 mmol) were dissolved in DMF (4 ml). DIEA (640 µl, 3.68 mmol) was added to the mixture at 0 °C and stirred at 0 °C for 2 h and r.t. overnight. The mixture was concentrated, diluted with $CHCl_3$, and washed successively with 4% $KHSO_4$ aq., saturated $NaHCO_3$ aq., and brine. The organic layer was dried over $MgSO_4$. The solution was concentrated and purified by silica gel chromatography (100 : 1 $CHCl_3$/MeOH) to provide **1** (358 mg, 39%): R_f 0.51 (10 : 1 chloroform/methanol). ^{1}H-NMR (400 MHz, $CDCl_3$): δ 7.23 (m, 5H, C_6H_5), 6.15 (d, 1H, J = 8.5 Hz, urethane NH), 5.14–5.07 (m, 1H, H–3′), 5.06–5.01 (d, 2H, J = 12.1 Hz, benzyl), 4.99 (t, 1H, J = 9.5 Hz, H-4′), 4.60 (s, 1H, amide), 4.21 (dd, 1H, J = 9.0, 12.6 Hz, H-6′a), 4.02–3.91 (2H, H-2′, 6′b), 3.69–3.59 (2H, H-1′, 2), 3.55–3.49 (m, 1H, H-5′), 2.33 (td, 1H, J = 11.6, 4.0 Hz, H-1), 2.09–2.00 (9H, 3 acetyl), 1.70–1.17 (8H, H-3, 4, 5, 6); MS (FAB, matrix: nitrobenzyl alcohol): *m/z* 649.3 (calcd. for $C_{32}H_{44}N_2O_{12}$ [(M+H)$^+$], *m/z* 649.3).

Boc-((GA(OAc))$_2$ACHC)-OCH$_2$C$_6$H$_5$ (2)

The Boc group of compound **1** (669 mg, 0.77 mmol) was removed with TFA and anisole. The obtained salt, Boc-GA(OAc)-OH (366 mg, 0.85 mmol), and HATU (349 mg, 0.92 mmol) were dissolved in DMF and stirred at 0 °C for 10 min. DIEA (265 µl, 1.52 mmol) was added to the mixture, and stirred at 0 °C for 3 h and at r.t. overnight. The mixture was concentrated, diluted with $CHCl_3$, and washed with 4% $KHSO_4$ aq, 4% $NaHCO_3$ aq, and brine. The organic layer was dried over $MgSO_4$. After evaporation of the solvent, the residue was washed with diisopropyl ether for three times to provide **2** (752 mg, 0.636 mmol, 83%): R_f 0.80 (10 : 1 chloroform/methanol). ^{1}H-NMR (400 MHz, $CDCl_3$): δ 7.31 (m, 5H, C_6H_5), 6.98 (1H, sugar amide NH), 6.73 (d, 1H, J = 8.9 Hz, cyclohexane amide NH) 5.10–4.97 (m, 4H, H-3, 3′, 4, 4′), 4.71 (1H, urethane NH), 4.24 (td, 1H, J = 5.5, 12.0 Hz, cyclohexane H-2), 4.15–3.97 (4H, H-6, 6′), 3.75–3.59 (m, 6H, 1, 1′, 2, 2′, 5, 5′), 2.31 (t, 1H, J = 10.52 Hz, cyclohexane H-1), 2.03 (18H, 6 acetyl), 1.26 (9H, Boc Me), 1.70–1.17 (cyclohexane 3–6); MS (FAB, matrix: nitrobenzyl alcohol): *m/z* 964.5 (calcd. for $C_{45}H_{61}N_3O_{20}$ [(M+H)$^+$], *m/z* 964.4).

Boc-((GA(OAc))$_2$ACHC)-OH (3)

A solution of compound **2** (752 mg, 0.636 mmol) in CH_2Cl_2 (156.6 ml) was subjected to catalytic hydrogenation in the presence of 20% palladium on activated carbon palladium black (235 mg) for 26 h. The catalyst was removed through cellite and the solvent was evaporated to yield the product **3** (508 mg, 0.576 mmol, 91%): R_f 0.53 (10 : 1 chloroform/methanol). ^{1}H-NMR (400 MHz, $CDCl_3$): δ 6.70 (1H, sugar amide NH), 6.63 (d, 1H, J = 8.0 Hz, cyclohexane amide NH), 5.67 (t, 1H, J = 10.0, H-3′), 5.32–5.14 (t, 1H, J = 9.8 Hz, H-3), 5.05–4.96(3H, H-4, 4′, urethane NH), 4.27–4.23, 4.06–3.97 (4H, H-6, 6′), 4.20–4.12 (3H, H-2, 2′, cyclohexane 2), 3.76–3.60 (2H, H-5, 5′), 1.45 (9H, Boc), 2.01 (18H, 6 acetyl), 1.26–1.10 (8H, H-3, 4, 5, 6); MS (FAB, matrix: nitrobenzyl alcohol): *m/z* 874.4 (calcd. for $C_{38}H_{55}N_3O_{20}$ [(M+H)$^+$], *m/z* 874.4).

CP2(OAc) (4)

The Boc group of compound **3** (37 mg, 0.042 mmol) was removed with TFA and anisole. The obtained salt, HATU (159.6 mg, 0.42 mmol), and HOAt (84 mg, 0.63 mmol) were dissolved in DMF (42 ml) and stirred at 0 °C for 10 min; then DIEA (134.4 µl, 0.756 mmol) in DMF (7.6 ml) was added dropwise, and the solution was stirred at 0 °C for 3 h, and at r.t. for 28 h. After evaporation, the residue was washed with methanol (several times) and hot

methanol (one time) to yield product **4** (31 mg, 95%): R_f 0.45 (10 : 1 chloroform/methanol). ^{1}H-NMR (400 MHz, dimethylsulfoxide-d6): δ 7.45 (d, 1H, J = 9.52, GAa amide NH), 7.17 (d, 1H, J = 8.00 Hz, GAa amide N*H*), 7.08 (d, 1H, J = 9.04, ACHC amide N*H*), 5.18 (t, 1H, J = 9.24 Hz, GAb 3), 5.08 (t, 1H, J = 9.8 Hz, GAa 3), 4.86 (t, 1H, J = 9.52, GAa 4), 4.80 (t, 1H, J = 9.52 Hz, GAb 4), 4.16–4.07 (5H, GAa 6, GAb 6, GAa 2), 4.40–4.01 (3H, GAa 1, GAb 1,2), 3.96–3.91 (3H, ACHC 2, GAa 5, GAb 5), 2.02–1.89 (18H, 6 acetyl), 1.79–1.11 (8H, ACHC 3, 4, 5, 6); MS (FAB, matrix: nitrobenzyl alcohol): *m/z* 778.4 (calcd. for $C_{33}H_{45}N_3O_{17}Na$ [(M+Na)$^+$], *m/z* 778.3).

CP2

Compound **4** (21.4 mg, 28.3 µmol) was dissolved in DMSO (3.1 ml), and 1N NaOH aq. (0.286 µl) was added to the solution. The mixture was stirred at 60 °C for 12 h. The mixture was neutralized with a 1 N HCl aq. The crude product was precipitated with acetone and diethyl ether. The residue was washed with acetone and water, and water was removed by freeze drying to yield the product **CP2** (10.5 mg, 74%): R_f 0.79 (Reversed-phase TLC, 50 : 5 : 1 methanol/formic acid/water). ^{1}H-NMR (400 MHz, formic acid-d2): δ 4.65(d, 1H, J = 6.00, GAab 1), 4.62 (d, 1H, J = 6.00, GAb 1), 4.50–4.45 (4H, GAab 2, 3), 4.16–3.83 (8H, GAab 4, 5, 6), 2.35 (td, 1H, J = 2.3, 10.1, ACHC NHCH), 1.96 (1H, ACHC COCH), 1.65–1.25 (8H, ACHC 3–6); MS (FAB, matrix: nitrobenzyl alcohol): *m/z* 526.2 (calcd. for $C_{21}H_{33}N_3O_{11}Na$ [(M+Na)$^+$], *m/z* 526.2).

Results and Discussion

Polarization Microscope Observation

CP2 is soluble in dimethylsulfoxide and formic acid, but pratically insoluble in water, *N*,*N*-dimethylformamide, and chloroform. The poor solubility is probably due to the facile formation of intermolecular hydrogen bonds. Rodlike crystals of CP2 were successfully obtained from a mixed solution of formic acid and diisopropyl ether. The crystals exhibited a highly ordered structure as shown by the polarization microscope observation with a sensitive tint plate (Figure 2), where a yellow-orange color (subtraction retardation) was observed in the case of parallel orientation between the long axis of the rodlike crystal and the z'-axis of the tint plate, and a blue color (addition retardation) in the case of their perpendicular orientation. The observation indicates that the short axis of the crystal has a larger refractive index than that of the long axis. In the previous reports of cyclo(ACHC)$_3$ [36] and cyclo(GA)$_3$ [38], the refractive index along the long axis was larger than that along the short axis due to the alignment of amide bonds along the long axis. In the case of CP2, hydrogen bonds between hydroxyl groups of neighboring PNTs may be formed and make the refractive index larger along the short axis.

Electron Diffraction Analysis

The CP2 crystals of 1.5–2 µm diameter and 15–40 µm length were subjected to the electron diffraction analysis. The electron beam was irradiated at the thin section of the specimen to obtain the diffraction pattern (Figure 3), which reveals a spacing of 4.8 Å along the long axis [29,30,39]. This length fits into the molecular thickness of the planar CP2 structure, and is consistent with the formation of columnar structure by CP2 stacking similar to the reports on other cyclic tri-β-peptides (Figure 1(c)) [29,30,36,38].

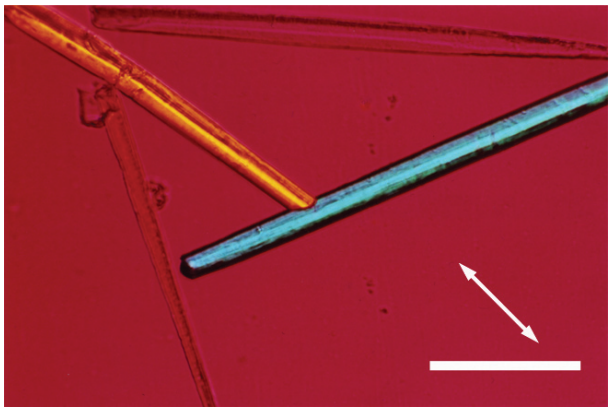

Figure 2. Optical microscopic observation at a cross-Nicol configuration of CP2 crystals. The double-headed allow shows the orientation of z'-axis of a sensitive tint plate. Bar = 10 µm.

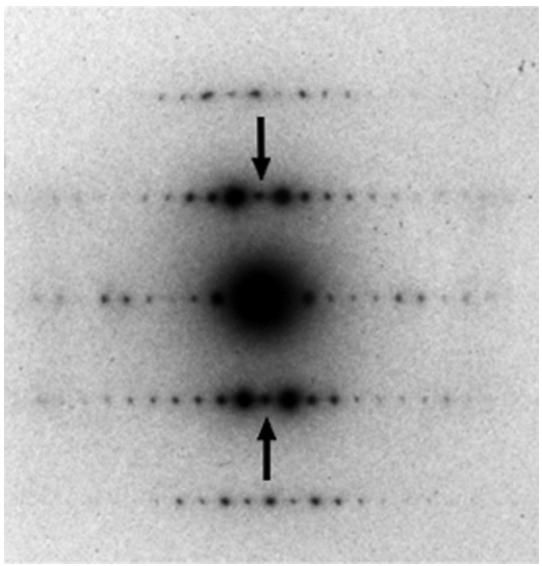

Figure 3. Electron diffraction pattern obtained with an incident electron beam perpendicular to the long axis of the rod-shaped assembly of CP2.

Notably, alternative light and dark spots along the short axis are observed in Figure 3, indicating the presence of spacing distances of 10.8 and 21.5 Å. The former length corresponds to the column diameter, which corresponds to the ring size of the planar CP2 structure. The latter length may reflect the triple bundle structure (Figure 1(d)), which was expected from the design of the amphiphilic CP2 that should associate into a trimer by facing the cyclohexyl units inward and exposing the pyranose moieties outside. The planar structure composed of three CP2 molecules should stack together via intermolecular hydrogen bond formation to give the triple bundle structure. The orientation of the columns in the bundle is either all parallel or two parallel and one opposite. In the case of cyclo(ACHC)$_3$, all parallel orientation was found in the crystal due to interdigitation of the cyclohexyl units. As diffraction spots appear at the intersections between the central meridian axis and the first layer lines [29,30], the columns should contain antiparallel alignment. The difference between CP2 and cyclo(ACHC)$_3$ is the multiple hydrogen-bond formation among PNTs, which may weaken the interdigitation effect of ACHC residues. However, details remain to be solved.

Journal of PeptideScience

IR Analysis

A solution of CP2 in formic acid and water (7/3 v/v) at 1.1×10^{-3} M was dried slowly on a CaF_2 plate in air and then *in vacuo*. An FT-IR spectrum of this white solid showed an amide I absorption (mainly C═O stretching mode) and an amide II absorption (mainly N–H bending and C–N stretching modes) at 1665 and 1565 cm^{-1} respectively. A sharp N–H stretching peak appeared at 3277 cm^{-1}, supporting that CP2 forms the columnar structure with homogeneous intermolecular hydrogen bonds. We estimated a stacking distance between CP2 molecules in the column from the N–H stretching frequency. According to the Krimm's analysis, the distance between nitrogen and oxygen atoms via the hydrogen bond is calculated to be *ca* 2.9 Å [36,39]. Further, the distance between nitrogen and oxygen atoms in the amide along the columnar axis is estimated to be 1.9 Å by geometry optimization. The sum of the two distances is the same as the axial spacing evaluated from the diffraction analysis of the CP2 crystal. CP2 thus shows a high tendency to form the columnar structure.

Fibrous Molecular Assembly from Formic Acid and Water

CP2 is a planar cyclic peptide with amide bonds oriented perpendicular to the ring to form PNT as shown in Figure 1(b) and (c). These PNTs tend to associate together to yield thick bundles despite the molecular design to induce the triple bundle formation. The facile association of PNTs may be due to the hydroxyl groups exposed on the outside of the triple bundle, which can readily make interbundle hydrogen bonds as adhesive forces. However, we have examined the effect of the peptide concentration during preparation of the crystalline molecular assemblies on molecular assembly sizes.

When a solution of CP2 in formic acid and water (7/3 v/v) at a concentration of 1.1×10^{-5} M was dried on a carbon-coated copper TEM grid, a rod-shaped assembly of *ca* 5 nm diameter, which corresponds to a nine-columnar (3× triple bundle) structure, was found as the dominant size even though the rod sizes varied widely (Figure 4). By increasing the peptide concentration to 1.1×10^{-4} M, a uniform fibrous assembly of *ca* 15 nm in diameter and more than 3 μm in length was obtained (Figure 5). When the concentration was raised up to 1.1×10^{-3} M, uniform and straight fibers of *ca* 100 nm in diameter and more than 60 μm in length were obtained (Figure 6). This observation contrasts those of winding fibers formed with β-sheet peptides [16–19] or amphiphilic block peptides [14,15,20,40]. The highly straight morphology of CP2 nanofibers might be due to the straight morphology of PNTs and the tight association between neighboring PNTs by multiple hydrogen-bond formation among hydroxyl groups.

Our initial purpose to obtain a thin bundle of PNTs is partially attained by formation of a rod-shaped assembly of *ca* 5 nm diameter, which should be composed of three of the initially designed triple bundles. By increasing the peptide concentrations in the assembly process, the number of triple bundles in the rod-shaped assemblies became higher, thus thickening the nanofibers to diameters of up to *ca* 100 nm. The reason for this thickening may be the multiple hydrogen-bond formation between hydroxyl groups on the PNT surfaces. We are looking for other functional groups to decorate the PNT surface to avoid the thickening effects and thus to attempt the preparation of PNT bundles with large dipole moments [41].

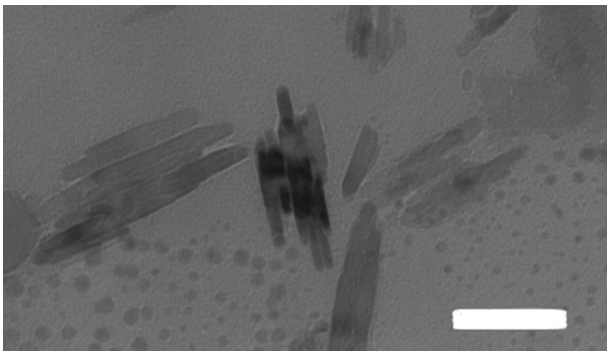

Figure 4. TEM image of molecular assembly prepared from 1.1×10^{-5} M solution of CP2 in formic acid and water (7/3 v/v). Bar = 50 nm.

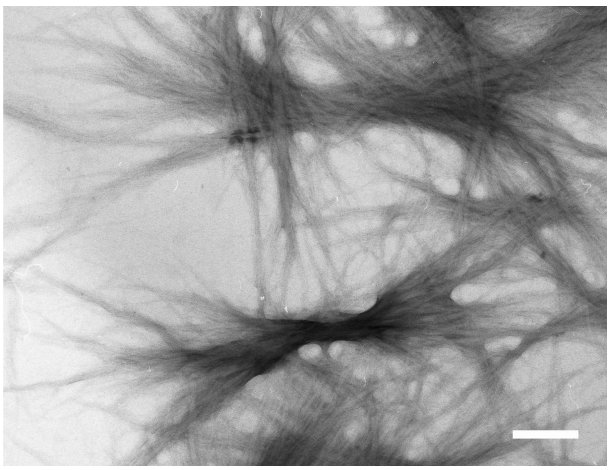

Figure 5. TEM image of molecular assembly prepared from 1.1×10^{-4} M solution of CP2 in formic acid and water (7/3 v/v). Bar = 300 nm.

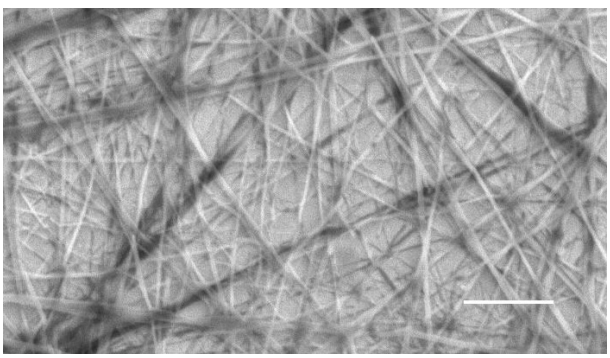

Figure 6. SEM image of molecular assembly prepared from 1.1×10^{-3} M solution of CP2. Bar = 5 μm.

Conclusion

A novel amphiphilic cyclic tri-β-peptide composed of two GAs and one ACHC was synthesized. This cyclic peptide was self-assembled into rodlike crystals or fibrous assemblies. TEM observation, electron diffraction analysis, and FT-IR spectroscopy indicated the PNT formation. The amphiphilic molecular structure contributed to association of three molecules into a trimeric unit. The molecular assemblies were stabilized by molecular stacking through hydrogen bonds between amides of the cyclic peptides

and interbundle hydrogen bonds through hydroxyl groups. By using a high concentration in the preparation, nanofibers of a highly straight form and composed of a higher number of triple bundles were obtained.

Acknowledgements

Authors thank Prof. J. Sugiyama and Dr. Y. Horikawa (Kyoto University Research institution for Sustainable Humanosphere) for their help in the TEM, SEM, and electron diffraction measurements.

References

1 Niu Z, Bruckman MA, Li S, Lee LA, Lee B, Pingali SV, Thiyagarajan P, Wang Q. Assembly of tobacco mosaic virus into fibrous and macroscopic bundled arrays mediated by surface aniline polymerization. *Langmuire* 2007; **23**: 6719–6724.
2 Horne WS, Ashkenasy N, Ghadiri MR. Modulating charge transfer through cyclic D, L-α-peptide self-assembly. *Chem. Eur. J.* 2005; **11**: 1137–1144.
3 Steinem C, Janshoff A, Vollmer MS, Ghadiri MR. Reversible photoisomerization of self-organized cylindrical peptide assemblies at air-water and solid interfaces. *Langmuir* 1999; **15**: 3956–3964.
4 Dzenls Y. Spinning contaneous fibers for nanotechnology. *Science* 2004; **304**: 1917–1919.
5 Lopez SF, Kim H, Choi EC, Delgado M, Granja JR, Khasanov A, Kraehenbuehl K, Weinberger DA, Wilcoxen KM, Ghadiri MR. Antibacterial agents based on the cyclic {D, L}-α-peptide architecture. *nature* 2001; **412**: 452–455.
6 Zhang Y, Lim CT, Ramakrishna S, Huang ZM. Recent development of polymer nanofibers for biomedical and biotechnological applications. *J. Mater. Sci.* 2005; **16**: 933–946.
7 Zhang S. Fabrication of novel biomaterials through molecular self-assembly. *Nat. Biotechnol.* 2003; **21**: 1171–1178.
8 Silva GA, Czeisler C, Niece KL, Beniash E, Harrington DA, Kessler JA, Stupp SI. Selective differentiation of neural progenitor cells by high-epitope density nanofibers. *Science* 2004; **303**: 1352–1355.
9 Ryadnov MG, Woolfson DN. Engineering the morphology of a self-assembling protein fibre. *Nat. Mater.* 2003; **2**: 329–332.
10 Zhao Y, Yokoi H, Tanaka M, Kinoshita T, Tan T. Self-assembled pH-responsive hydrogels composed of the RATEA16 peptide. *Biomacromolecules* 2008; **9**: 1511–1518.
11 Murasato K, Matsuura K, Kimizuka N. Self-assembly of nanofiber with uniform width from wheel-type trigonal- beta-sheet-forming peptide. *Biomacromolecules* 2008; **9**: 913–918.
12 Yang Y, Khoe U, Wang X, Horii A, Yokoi H, Zhang S. Designer self-assembling peptide nanomaterials. *Nano Today* 2009; **4**: 193–210.
13 Yang H, Fung S, Pritzker M, Chen P. Surface-assisted assembly of an ionic-complementary peptide: controllable growth of nanofibers. *J. Am. Chem. Soc.* 2007; **129**: 12200–12210.
14 Lim Y, Moon K, Lee M. Recent advances in functional supramolecular nanostructures assembled from bioactive building blocks. *Chem. Soc. Rev.* 2009; **38**: 925–934.
15 Zhao X, Zhang S. Designer self-assembling peptide materials. *Macromol. Biosci.* 2007; **7**: 13–22.
16 Qiu F, Chen Y, Zhao X. Comparative studies on the self-assembling behaviors of cationic and catanionic surfactant-like peptides. *J. Colloid and Interface Sci.* 2009; **336**: 477–484.
17 Marini DM, Hwang W, Lauffenburger DA, Zhang S, Kamm RD. Left-handed helical ribbon intermediates in the self-assembly of a β-sheet peptide. *Nano lett* 2002; **2**: 295–299.
18 Aggeli A, Nyrkova IA, Bell M, Harding R, Carrick L, McLeish TCB, Semenov AN, Boden N. Hierarchical self-assembly of chiral rod-like molecules as a model for peptide β-sheet tapes, ribbons, fibrils, and fibers. *Proc. Natl. Acad. Sci.* 2001; **98**: 11857–11862.
19 Aggeli A, Bell M, Boden N, Keen JN, Knowles PF, McLeish TCB, Pitkeathly M, Radford SE. Responsive gels formed by the spontaneous self-assembly of peptides into polymeric β-sheet tapes. *Nature* 1997; **386**: 259–262.
20 Hartgerink JD, Beniash E, Stupp SI. Self-assembly and mineralization of peptide-amphiphile nanofibers. *Science* 2001; **294**: 1684–1688.
21 Clark TD, Buriak JM, Kobayashi K, Isler MP, McRee DE, Ghadiri MR. Cylindrical β-sheet peptide assemblies. *J. Am. Chem. Soc.* 1998; **120**: 8949–8962.
22 Ghadiri MR, Granja JR, Milligan RA, McRee DE, Khazanovich N. Self-assembling organic nanotubes based on a cyclic peptide architecture. *Nature* 1993; **366**: 324–327.
23 Horne WS, Stout CD, Ghadiri MR. A heterocyclic peptide nanotube. *J. Am. Chem. Soc.* 2003; **125**: 9372–9376.
24 Rapaport H, Kim HS, Kjaer K, Howes PB, Cohen S, Nielsen JA, Ghadiri MR, Leiserowitz L, Lahav M. Crystalline cyclic peptide nanotubes at interfaces. *J. Am. Chem. Soc.* 1999; **121**: 1186–1191.
25 Hartgerink JD, Granja JR, Milligan RA, Ghadiri MR. Self-assembling peptide nanotubes. *J. Am. Chem. Soc.* 1996; **118**: 43–50.
26 Seebach D, Matthews JL, Meden A, Wessels T, Baerlocher C, McCusker LB. Cyclo-beta- peptides: structure and tubular stacking of cyclic tetramers of 3-aminobutanoic acid as determined from powder diffraction data. *Helv. Chim. Acta.* 1997; **80**: 173–182.
27 Clark TD, Buehler LK, Ghadiri MR. Self-assembling cyclic β-peptide nanotubes as artificial transmmembrane ion channels. *J. Am. Chem. Soc.* 1998; **120**: 651–656.
28 Hartgerink JD, Clark TD, Ghadiri MR. Peptide nanotubes and beyond. *Chem. Eur. J.* 1998; **4**: 1367–1372.
29 Fujimura F, Hirata T, Horikawa Y, Sugiyama J, Morita T, Kimura S. Columnar assembly of cyclic β-amino acid functionalized with pyranose rings. *Biomacromolecules* 2006; **7**: 2394–2400.
30 Fujimura F, Hirata T, Kimura S. Construction of nanotubes and their bundles from cyclic β-peptide. *Pept. Sci.* 2006; 360–360.
31 Wang C, Stewart RJ, KopeŠek J. Hybrid hydrogels assembled from synthetic polymers and coiled-coil protein domains. *Nature* 1999; **397**: 417–420.
32 Petka WA, Harden JL, McGrath KP, Wirtz D, Tirrell DA. Reversible hydrogels from self-assembling artificial proteins. *Science* 1998; **281**: 389–392.
33 Zimenkov Y, Conticello VP, Guob L, Thiyagarajan P. Rational design of a nanoscale helical scaffold derived from self-assembly of a dimeric coiled coil motif. *Tetrahedron* 2004; **60**: 7237–7246.
34 Paramonov SE, Jun HW, Hartgerink JD. Self-assembly of peptide-amphiphile nanofibers: the roles of hydrogen bonding and amphiphilic packing. *J. Am. Chem. Soc.* 2006; **128**: 7291–7298.
35 Nowak AP, Breedveld V, Pakstis L, Ozbas B, Pine DJ, Pochan D, Deming TJ. Rapidly recovering hydrogel scaffolds from self-assembling diblock copolypeptide amphiphiles. *Nature* 2002; **417**: 424–428.
36 Fujimura F, Fukuda M, Sugiyama J, Morita T, Kimura S. Parallel assembly of dipolar columns composed of a stacked cyclic tri-β-peptide. *Org. Biomol. Chem.* 2006; **4**: 1896–1901.
37 Suhara Y, Hildreth JEK, Ichikawa Y. Synthesis of a new carbohydrate mimettics: ''carbopeptide'' containing A C-1 carboxylate and C-2 amono group. *Tetrahedron Lett.* 1996; **37**: 1575–1578.
38 Fujimura F, Horikawa Y, Sugiyama J, Morita T, Kimura S. Double assembly composed of lectin association with columnar molecular assembly of cyclic tri-β-peptide having sugar units. *Biomacromolecules* 2007; **8**: 611–616.
39 Krimm S, Bandekar J. in *Adv. Protein Chem.* (Eds: Anifinsen CB, Edsall JT, Richards FM) Academic Press: Orlando, 1986; pp 181–364.
40 Kanzaki T, Horikawa Y, Makino A, Sugiyama J, Kimura S. Nanotube and three-way nanotube formation with nonionic amphiphilic block peptides. *Macromol. Biosci.* 2008; **8**: 1026–1033.
41 Kimura S. Molecular dipole engineering: New aspects of molecular dipoles in molecular architecture and their fuctions. *Org. Biomol. Chem.* 2008; **6**: 1143–1148.

